Virologica Sinica 39 (2024) 403–413

Contents lists available at ScienceDirect

Virologica Sinica

journal homepage: www.keaipublishing.com/en/journals/virologica-sinica
www.virosin.org

Research Article

Pseudorabies virus manipulates mitochondrial tryptophanyl-tRNA synthetase 2 for viral replication

Xiu-Qing Li [a,b,c,1], Meng-Pan Cai [a,b,c,1], Ming-Yang Wang [a,b,c], Bo-Wen Shi [g], Guo-Yu Yang [b,c,e], Jiang Wang [a,b,c,f,*], Bei-Bei Chu [a,b,c,d,e,f,*], Sheng-Li Ming [a,b,c,*]

[a] College of Veterinary Medicine, Henan Agricultural University, Zhengzhou 450046, China
[b] Key Laboratory of Animal Biochemistry and Nutrition, Ministry of Agriculture and Rural Affairs, Zhengzhou 450046, China
[c] Key Laboratory of Veterinary Biotechnology of Henan Province, Henan Agricultural University, Zhengzhou 450046, China
[d] Longhu Advanced Immunization Laboratory, Zhengzhou 450046, China
[e] International Joint Research Center of National Animal Immunology, Henan Agricultural University, Zhengzhou 450046, China
[f] Ministry of Education Key Laboratory for Animal Pathogens and Biosafety, Zhengzhou 450046, China
[g] School of Basic Medicine, Chongqing Medical University, Chongqing 400016, China

ARTICLE INFO

Keywords:
Pseudorabies virus
WARS2
Innate immunity
Protein synthesis
Lipid synthesis

ABSTRACT

The pseudorabies virus (PRV) is identified as a double-helical DNA virus responsible for causing Aujeszky's disease, which results in considerable economic impacts globally. The enzyme tryptophanyl-tRNA synthetase 2 (WARS2), a mitochondrial protein involved in protein synthesis, is recognized for its broad expression and vital role in the translation process. The findings of our study showed an increase in both mRNA and protein levels of WARS2 following PRV infection in both cell cultures and animal models. Suppressing WARS2 expression via RNA interference in PK-15 cells led to a reduction in PRV infection rates, whereas enhancing WARS2 expression resulted in increased infection rates. Furthermore, the activation of WARS2 in response to PRV was found to be reliant on the cGAS/STING/TBK1/IRF3 signaling pathway and the interferon-alpha receptor-1, highlighting its regulation via the type I interferon signaling pathway. Further analysis revealed that reducing WARS2 levels hindered PRV's ability to promote protein and lipid synthesis. Our research provides novel evidence that WARS2 facilitates PRV infection through its management of protein and lipid levels, presenting new avenues for developing preventative and therapeutic measures against PRV infections.

1. Introduction

The pseudorabies virus (PRV), known alternatively as porcine herpesvirus 1 or Aujeszky's disease virus, is classified within the alphaherpesvirus family (Mettenleiter, 1999). Characterized by its sizable linear double-stranded DNA genome, PRV encodes upwards of 70 functional proteins and is prevalent among pigs, its primary hosts, as well as various other vertebrates (Pomeranz et al., 2005; Wozniakowski and Samorek-Salamonowicz, 2015). The virus is notorious for inciting devastating diseases and inflicting significant economic detriment globally (Wozniakowski and Samorek-Salamonowicz, 2015). Recent research has unveiled the troubling capability of PRV variants to infect humans directly, inflicting serious harm to both the nervous and respiratory systems and underscoring the risk of this virus breaching species barriers (Ai et al., 2018; Wong et al., 2019; Yang et al., 2019). This body of evidence points to the fact that the impact of PRV extends beyond agricultural confines, posing a looming threat to public health.

Mitochondrial aminoacyl-tRNA synthetases (mtARSs) are essential enzymes that are ubiquitously expressed and covalently attach amino acids to their corresponding tRNA molecules during the translation of mitochondrial genes. Harmful mutations in mtARS genes can lead to various phenotypes, and different mtARS mutations often result in distinct clinical manifestations (Burke et al., 2018). Tryptophanyl-tRNA synthetase 2 (WARS2) is a type of mtARS. Human genome-wide association studies have identified heritable WARS2 gene expression in breast cancers, and the WARS2 locus has been associated with cardio-metabolic phenotypes (Heid et al., 2010; Curtis et al., 2012). WARS2 possesses

* Corresponding authors.
E-mail addresses: mingsl911102@163.com (S.-L. Ming), chubeibei@henau.edu.cn (B.-B. Chu), wangjiang@henau.edu.cn (J. Wang).
[1] Xiu-Qing Li and Meng-Pan Cai contributed equally to this work.

https://doi.org/10.1016/j.virs.2024.04.003
Received 10 October 2023; Accepted 11 April 2024
Available online 16 April 2024

angiogenic properties both within and beyond the cardiac context (Liu et al., 2010), and given its association with common human diseases, it may have translational relevance (Wang et al., 2016). Patients harboring biallelic WARS2 variants may exhibit symptoms of neonatal or infantile mitochondrial disease, as well as dopamine-responsive early-onset Parkinson's disease and progressive myoclonus-ataxia (Burke et al., 2018; Tarnopolsky et al., 2020; Skorvanek et al., 2022).

Viruses are uniquely dependent on the cellular mechanisms of their hosts for their own reproduction (Wang and Li, 2012; Walsh et al., 2013). Regardless of their diverse sizes, structural compositions, complexities, and genetic functions, their survival hinges entirely on hijacking the protein production systems within host cells (Sánchez et al., 2013; Walsh et al., 2013). Beyond their role as energy stores, lipids are pivotal in shaping the fluidity and architecture of cellular membranes (Lorizate and Krausslich, 2011). For their lifecycle completion, viruses exploit host cellular proteins and lipids (Wang and Li, 2012). The process of metabolic remodeling is crucial for viruses to amplify their biomass, enabling the amplification of their genetic material and the assembly of new virus particles (Allen et al., 2022). Prior to our study, the influence of WARS2 on the metabolic pathways affecting PRV growth had not been explored. Our exploration revealed that reducing WARS2 levels curtailed the PRV-triggered spike in protein and lipid production, consequently diminishing PRV growth. This finding highlights the critical role of WARS2 in PRV infection processes.

2. Materials and methods

2.1. Reagents

TRIzol Reagent (9108, TaKaRa), PrimeScript RT reagent kit (RR047A, TaKaRa) SYBR Premix Ex Taq (RR820A, TaKaRa) were purchased from TaKaRa (Otsu, Shiga, Japan); Oil red O (O0625), cycloheximide (CHX, 239763) and RNase inhibitor (3335399001) were purchased from Sigma-Aldrich (MO, USA); a lab assay nonessential fatty acid (294-63601) assay kit for FFAs was from Wako Bioproducts (VA, USA), and a TG assay kit (E1013) and TC assay kit (E1015) were purchased from Applygen Technologies Inc. (Beijing, China). Enhanced ATP Assay Kit (S0027) was purchased form Beyotime (shanghai, China). Acetyl-CoA Content Assay Kit (BC0980) was purchased form Solarbio (Beijing, China).

2.2. Antibodies

Anti-ACACA (#3676), anti-p-ACACA (#11818) and anti-p-eIF2α (#3398) antibodies were purchased from Cell Signaling Technology (MA, USA); anti-WARS2 (13944-1-AP), anti-cGAS (26416-1-AP), anti-STING (19851-1-AP), anti-TBK1 (28397-1-AP), anti-IFR3 (11312-1-AP), anti-IFNAR1 (13083-1-AP), anti-eIF2α (11170-1-AP) and anti-β-actin (20536-1-AP), anti-NDUFA9 (20312-1-AP), anti-SDHA (14865-1-AP) and anti-COXI (13393-1-AP) were purchased from Proteintech (Wuhan, China); anti-FASN (ab22759) was purchased from Abcam (MA, USA); anti-FLAG (F3165), anti-puromycin (MABE343) and anti-HMGCR (MABS1233) was purchased from Sigma-Aldrich (MO, USA); anti-p-HMGCR (bs-4063R) was purchased from Bioss (MA, USA); horseradish peroxidase (HRP)-conjugated donkey anti-mouse IgG (715-035-150) and anti-rabbit IgG (711-035-152) were purchased from Jackson Immuno Research Laboratories (PA, USA). Antiserum against PRV gB was generated by immunizing mice with purified recombinant gB. The antibodies were used at dilutions of 1:500 for immunofluorescence staining and 1:1000 for immunoblotting analysis.

2.3. Mice

Female 6 to 8-week-old BALB/c mice were purchased from the Center of Experimental Animals of Zhengzhou University (Zhengzhou, China) and maintained in a specific pathogen-free animal facility according to the Guide for the Care and Use of Laboratory Animals and the related ethical regulations instilled at Henan Agricultural University.

2.4. Cells and viruses

Porcine kidney epithelial PK-15 cells (CCL-33, ATCC, MD, USA) and HE293T cells (CRL-11268, ATCC) were grown in monolayers at 37 °C under 5% CO_2 in DMEM (10566-016, Gibco, NY, USA) supplemented with 10% FBS (10099141C, Gibco, MA, USA), 100 U/mL penicillin, and 100 μg/mL streptomycin sulfate (B540732, Sangon, Shanghai, China). *cGAS*$^{-/-}$, *STING*$^{-/-}$, *TBK1*$^{-/-}$, *IRF3*$^{-/-}$ *and IFNAR1*$^{-/-}$ PK-15 cells were used as previously described (Wang et al., 2020). Briefly, lentiviruses-mediated CRISPR/Cas9 technology was used to generate gene knockout cell lines. PK15 cells were infected with the lentiviruses and subsequently selected with puro (4 μg/mL) for seven days. Single clonal knockout cells were obtained by serial dilution and verified by Sanger sequencing and immunoblotting analysis.

The virulent PRV isolate QXX (PRV-QXX) was kindly donated by Yong-Tao Li from the College of Veterinary Medicine, Henan Agricultural University (Li et al., 2015). The recombinant PRV strain of PRV-GFP, derived from the PRV Hubei strain with the *TK* gene replaced by a GFP expression cassette from the pEGFP-N1 plasmid, was kindly donated by Han-Zhong Wang from Wuhan Institute of Virology, Chinese Academy of Sciences (Xu et al., 2012). Viral titers were determined using the 50% tissue culture infective dose ($TCID_{50}$) assay, which was calculated via the Reed-Muench method.

2.5. Plasmids

Full-length porcine WARS2 cDNA was amplified by polymerase chain reaction. WARS2 cDNA was cloned into pEGFP-C1 and p3 × Flag-CMV-10 expression plasmids to generate GFP-WARS2 and FLAG-WARS2. FLAG-WARS2 mut (48–54) was a mutant form of full-length WARS2 in which amino acids 48 to 54 were mutated to alanine. FLAG-WARS2 Δ(aa.1–18) referred to truncating amino acids 1–18 of the full-length WARS2. All DNA constructs were verified with DNA sequencing. All plasmids were transfected with Lipofectamine 3000 (L3000015, Invitrogen, NY, USA) according to the manufacturer's instructions.

2.6. Cell viability assay

Cell viability was evaluated using a cell Counting kit-8 (CCK-8) according to the manufacturer's instructions (GK3607, Dingguo, Beijing). Briefly, the cells were seeded into 96-well plates at a density of 0.8×10^4 per well for 24 h. CCK-8 (10 μL) was then added to each well, and the cells were incubated at 37 °C for 3 h. The absorbance was detected at 450 nm with a microplate reader (VARIOSKAN FLASH, ThermoFisher Scientific).

2.7. Flow cytometry assay

A flow cytometry assay was performed as previously described (Gack et al., 2020). Briefly, PK-15 cells were infected with PRV-GFP [multiplicity of infection (MOI) = 1] for 20 h. Cells were digested with trypsin-EDTA (25200072, Gibco, MA, USA), collected by centrifugation, and suspended in PBS. The percentage of GFP-positive cells was measured by flow cytometry using a Beckman CytoFLEX instrument. All data were analyzed with CytExpert software 2.0.

2.8. qRT-PCR

Total RNA was extracted using TRIzol Reagent (TaKaRa) and reverse-transcribed with a PrimeScript RT reagent kit (TaKaRa). qRT-PCR was performed in triplicate using SYBR Premix Ex Taq (TaKaRa). Data were normalized to the expression of the control gene encoding β-actin. The relative changes in expression were calculated using the $2^{-\Delta\Delta CT}$ method.

The primer sequences used for qRT-PCR analysis are shown in Supplementary Table S1.

2.9. Immunoblotting analysis

The cells were lysed in RIPA buffer (50 mmol/L Tris–HCl, pH 8.0, 150 mmol/L NaCl, 1% Triton X-100, 1% sodium deoxycholate, 0.1% SDS, and 2 mmol/L $MgCl_2$) supplemented with a protease and phosphatase inhibitor cocktail (HY-K0010 and HY-K0022, MedChemExpress). Protein samples were separated by SDS-PAGE and transferred to polypropylene fluoride membranes (C3117, Millipore, MA, USA). After a 30 min incubation in 5% nonfat milk (A600669, Sangon Biotech), the membrane was incubated with the primary antibody overnight at 4 °C followed by an incubation with the appropriate HRP-conjugated secondary antibody for 1 h at room temperature. The target proteins were detected with Luminata Crescendo immunoblotting HRP substrate (WBLUR0500, Millipore) on a GE AI600 imaging system.

2.10. RNAi

Lentivirus-mediated gene silencing was conducted as previously described (Wang et al., 2019). Briefly, shRNAs (Scramble: GCCACAACGTCTATATCATGG; shWARS2-1: CTTAATTGGTGCAAATCTCTC; shWARS2-2: CTCTTAATTGGTGCAAATCTC) were synthesized as double-stranded oligonucleotides, cloned into the pLKO.1 vector and co-transfected with packaging plasmids pMD2.G and psPAX2 into HE293T cells. Lentiviruses were harvested at 48 h post-transfection and used to infect cells that were then selected with puro (4 μg/mL) for seven days. Knockdown efficiency was determined by qRT-PCR or immunoblotting analysis.

2.11. Determination of intracellular FFAs, TG, and TC

The cell lysates were extracted with a syringe needle in 250 μL RIPA buffer and centrifuged at 12,000 ×*g* for 5 min at 4 °C. The total lipids in 200 μL lysate were extracted by the addition of 100 μL chloroform–methanol (2:1, v/v) mixture. The extract was evaporated until dry and dissolved in 50 μL of TRB (100 mmol/L KH_2PO_4, 100 mmol/L K_2HPO_4, 5 mmol/L sodium cholate, 50 mmol/L NaCl, 0.1% Triton X-100, pH 7.4) for the FFA, TG, and TC assays. FFA (Wako), TG (Applygen), and TC (Applygen) were measured with biochemical assay kits in accordance with the manufacturer's protocols. The values were normalized to the total cellular protein content.

2.12. Oil red O staining

The cells were fixed in 4% paraformaldehyde for 30 min and incubated in Oil red O (3 μg/mL) for 15 min. The cells were washed with 70% alcohol for 5 s to remove any background stain, rinsed in double-distilled Millipore water, counterstained with Harris hematoxylin, washed, mounted, and observed under a light microscope. The LD number was determined using the ImageJ "analyze particles" function (areas of particles <0.01 mm^2 were excluded).

2.13. Polysome profile analysis

Methodology reference to previous reports (Han et al., 2020). Mock or PRV-QXX-infected (MOI = 1) PK-15 cells were incubated with 0.1 mg/mL CHX (Sigma-Aldrich) for 5 min at 37 °C to arrest the ribosome at specific times after infection. The cells were then lysed in polysome extraction buffer (20 mmol/L Tris-HCl [pH 7.5], 5 mmol/L $MgCl_2$, 100 mmol/L KCl, 1% Triton X-100, 0.1 mg/mL CHX, 1 × protease inhibitor cocktail, and 50 U/mL RNase inhibitor). The cell lysates were centrifuged at 15,000 ×*g* for 10 min at 4 °C, and the supernatants were resolved on a linear 10%-to-50% sucrose gradient (composed of 20 mmol/L Tris-HCl [pH 7.5], 5 mmol/L $MgCl_2$, and 100 mmol/L KCl) by centrifugation at 35,000 rpm at 4 °C for 3 h in a Beckman SW40 Ti rotor. After centrifugation, the fractions were collected, and the optical density was measured at a wavelength of 254 nm (OD_{254}) with varioskan flash (Thermo, USA). Methodology reference to previous reports (Han et al., 2020).

2.14. Statistical analysis

Data are representative of at least three independent experiments for quantitative analyses and expressed as the means ± standard errors of the means. All statistical analyses were performed with a two-tailed Student's *t*-test. Significant differences relative to the corresponding controls were accepted at $P < 0.05$.

3. Results

3.1. WARS2 expression is increased during PRV infection

The role of WARS2 during PRV infection was explored by assessing its expression in mice exposed to PRV. Mice were exposed to either a mock infection or an intranasal PRV-QXX strain for three days, followed by the measurement of WARS2 mRNA and protein levels in tissues such as the kidney, brain, lung, and liver through quantitative real-time PCR (qRT-PCR) and immunoblotting analysis, respectively. Relative to the mock-infected group, a notable rise in WARS2 mRNA levels was observed in all tissues post-PRV infection (Fig. 1A). A similar upward trend in WARS2 protein quantities was detected in these organs (Fig. 1B–D). For *in vitro* investigation, PK-15 cells were infected with PRV-QXX over a time course of 0–24 h, displaying an elevation in both WARS2 mRNA and protein expressions (Fig. 1E, F). Further, the study evaluated the effect of PRV infection on WARS1 and EARS2, another mitochondrial aminoacyl tRNA synthetase. The qRT-PCR outcomes revealed that the expression levels of WARS1 and EARS2 remained unchanged by PRV infection (Fig. 1G, H). These observations indicate an upregulation of WARS2 expression following PRV infection.

3.2. WARS2 expression is regulated by type I interferon (IFN) and cGAS/STING/TBK1/IRF3 pathways

Following the observation of enhanced WARS2 expression during PRV infection, we sought to elucidate whether this expression modulation was mediated via the type I interferon (IFN) signaling pathway. To this end, PK-15 cells were subjected to various stimuli, including IFN-β, HT-DNA, poly (I:C), and poly (dA:dT); all of which resulted in increased mRNA levels of WARS2 and the IFN-stimulated gene 15 (ISG15) (Fig. 2A–D). Previous investigations have identified the involvement of porcine cyclic GMP-AMP (cGAMP) synthase (cGAS) and components downstream, such as the stimulator of interferon genes protein (STING), TANK-binding kinase 1 (TBK1), and IFN regulatory factor 3 (IRF3), in the activation of type I IFN in response to PRV infection (Wang et al., 2015). CRISPR/Cas9 technology was employed to generate *cGAS*$^{-/-}$, *STING*$^{-/-}$, *TBK1*$^{-/-}$, *IRF3*$^{-/-}$, and *IFNAR1*$^{-/-}$ PK-15 cell lines (Wang et al., 2020). The efficacy of these genetic modifications was verified via immunoblotting analysis (Fig. 2E). A time-dependent increase in WARS2 expression was observed in PK-15 cells upon PRV-QXX infection (Fig. 2F). However, such induction was not present in the *cGAS*$^{-/-}$, *STING*$^{-/-}$, *TBK1*$^{-/-}$, *IRF3*$^{-/-}$, and *IFNAR1*$^{-/-}$ PK-15 cells (Fig. 2F), indicating that the cGAS/STING/TBK1/IRF3 innate immune and IFN signaling axes are indispensable for the PRV-induced expression of WARS2.

3.3. WARS2 knockdown inhibits PRV infection

To investigate the presumptive involvement of WARS2 in PRV infection, RNA interference (RNAi) technology was utilized to suppress WARS2 expression by introducing short-hairpin RNA (shRNA) into

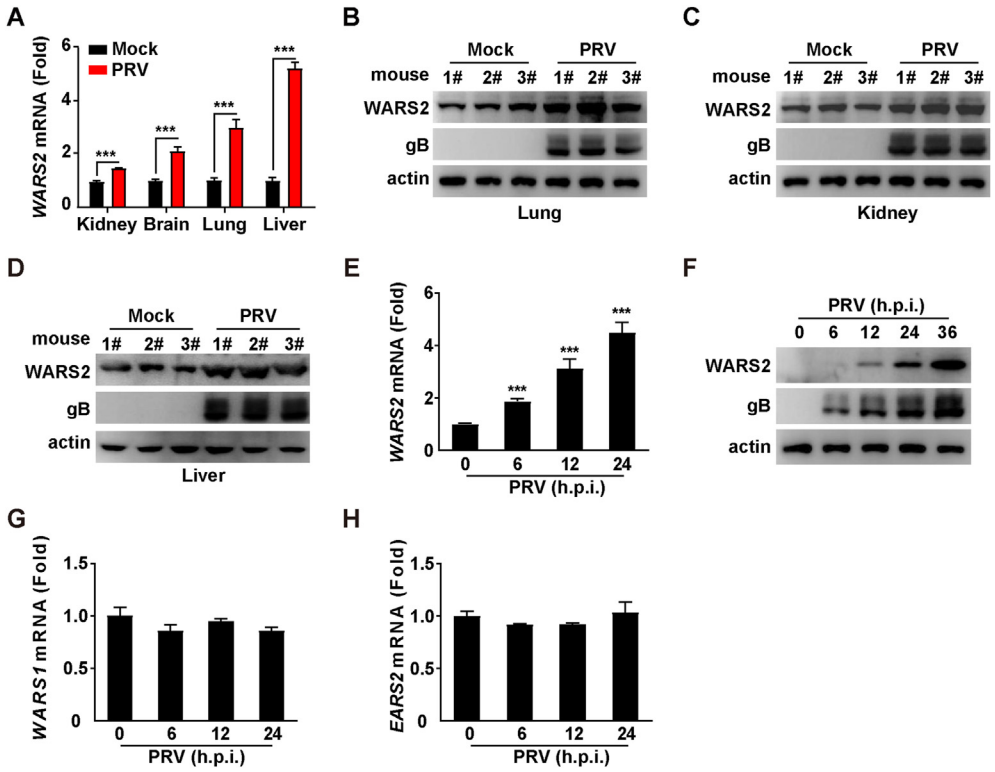

Fig. 1. WARS2 expression is unregulated by PRV infection. **A** Murine models were either subjected to a mock infection or intranasal administration of PRV-QXX at a concentration of 5×10^3 $TCID_{50}$ within a 50 μL volume per specimen, maintained for a duration of 3 days. Subsequently, the expression levels of WARS2 mRNA within the renal, cerebral, pulmonary, and hepatic tissues were quantitatively analyzed via qRT-PCR (n = 3 per treatment group). ***$P < 0.001$. **B–D** Following the procedural steps outlined in section (**A**), the expression of WARS2 and PRV glycoprotein B (gB) within the pulmonary (**B**), renal (**C**), and hepatic (**D**) tissues were evaluated utilizing immunoblotting analysis (n = 3 per treatment group). **E** PK-15 cells were exposed to PRV-QXX with a MOI of 1 for 0–24 h. The expression level of WARS2 mRNA was subsequently quantified through qRT-PCR analysis. ***$P < 0.001$. **F** PK-15 cells were exposed to PRV-QXX with a MOI of 1 for 0–24 h. The protein expressions of WARS2 and gB were evaluated utilizing immunoblotting analysis. **G–H** PK-15 cells exposed to PRV-QXX with a MOI of 1 for 0–24 h. The expression levels of WARS1 (**G**) and EARS2 (**H**) mRNA were quantitatively analyzed via qRT-PCR.

PK-15 cells prior to infection with recombinant strains of PRV-GFP and PRV-QXX. The efficiency of WARS2 downregulation by the two selected shRNAs was validated through both qRT-PCR and immunoblotting (Fig. 3A and B). Furthermore, it was observed that the knockdown of WARS2 did not adversely impact the morphological characteristics or survival of PK-15 cells (Fig. 3C and D). Meanwhile, knockdown of WARS2 did not affect the expressions of cGAS, STING, TBK1, IRF3 and IFNAR 1 (Fig. 3E).

Subsequent investigations focused on viral replication dynamics in PK-15 cells, employing control (scramble), shWARS2-1, and shWARS2-2 cell lines, following infection with PRV-GFP. These dynamics were assessed via fluorescence microscopy and flow cytometry, revealing a significant diminution in GFP fluorescence in cells with WARS2 silenced as opposed to the control cells (Fig. 3F and G). Infection trials were extended to cover PRV-QXX strain, with the replication rates quantified through the detection of PRV glycoprotein B (gB) expression levels via immunoblotting and mRNA levels of PRV gB and thymidine kinase (TK) through qRT-PCR analysis. These analyses indicated a reduction in PRV gB protein as well as gB and TK mRNA levels in shWARS2-1 and shWARS2-2 cells compared to scramble controls (Fig. 3H and I). Moreover, viral titer assessments revealed reduced viral loads in WARS2-suppressed cells (Fig. 3J). Collectively, these results imply that WARS2 silencing suppresses the proliferation of PRV in PK-15 cells.

3.4. *WARS2 overexpression promotes PRV infection*

To elucidate the contribution of WARS2 to PRV infection further, PK-15 cells were transfected with either an empty vector or varying concentrations of a plasmid harboring the FLAG-tagged WARS2 construct for a duration of 24 h, followed by an infection with PRV-GFP. Analytical outcomes, derived from fluorescence microscopy and flow cytometry evaluations, illustrated that cells with enforced expression of WARS2 exhibited enhanced GFP fluorescence compared to those receiving the empty vector (control group), signifying that WARS2 augmentation facilitated PRV-GFP infectivity (Fig. 4A and B). The investigation extended to measuring the impact of elevated WARS2 levels on PRV gB expression, utilizing immunoblotting techniques. Results depicted in Fig. 4C demonstrate an upsurge in PRV gB expression in cells transduced with the FLAG-WARS2 construct. In addition, PK-15 cells overexpressing FLAG-WARS2 showed elevated mRNA levels of PRV gB and TK relative to control cells (Fig. 4D). Viral titer assessments further substantiated that WARS2 overexpression potentiated viral replication (Fig. 4E). These findings collectively indicate that WARS2 upregulation is conducive to the proliferation of PRV.

3.5. *WARS2 knockdown inhibits protein synthesis and reduces the levels of cellular oxidative phosphorylation, ATP and Acetyl-Coenzyme A (acetyl-CoA) during PRV infection*

To elucidate the contribution of WARS2 to PRV proliferation, cellular extracts from either uninfected (mock) or PRV-infected PK-15 cells were subjected to sucrose gradient fractionation, facilitating the separation of ribosomal subunits (40S and 60S), monosomes (80S), and polysomes. Ribosomal profiling assessments revealed an augmentation in polysome abundance after PRV infection, a phenomenon not observed in cells subjected to WARS2 depletion (Fig. 5A). To further delineate WARS2's involvement in protein biosynthesis, a transient puromycin (puro) pulse

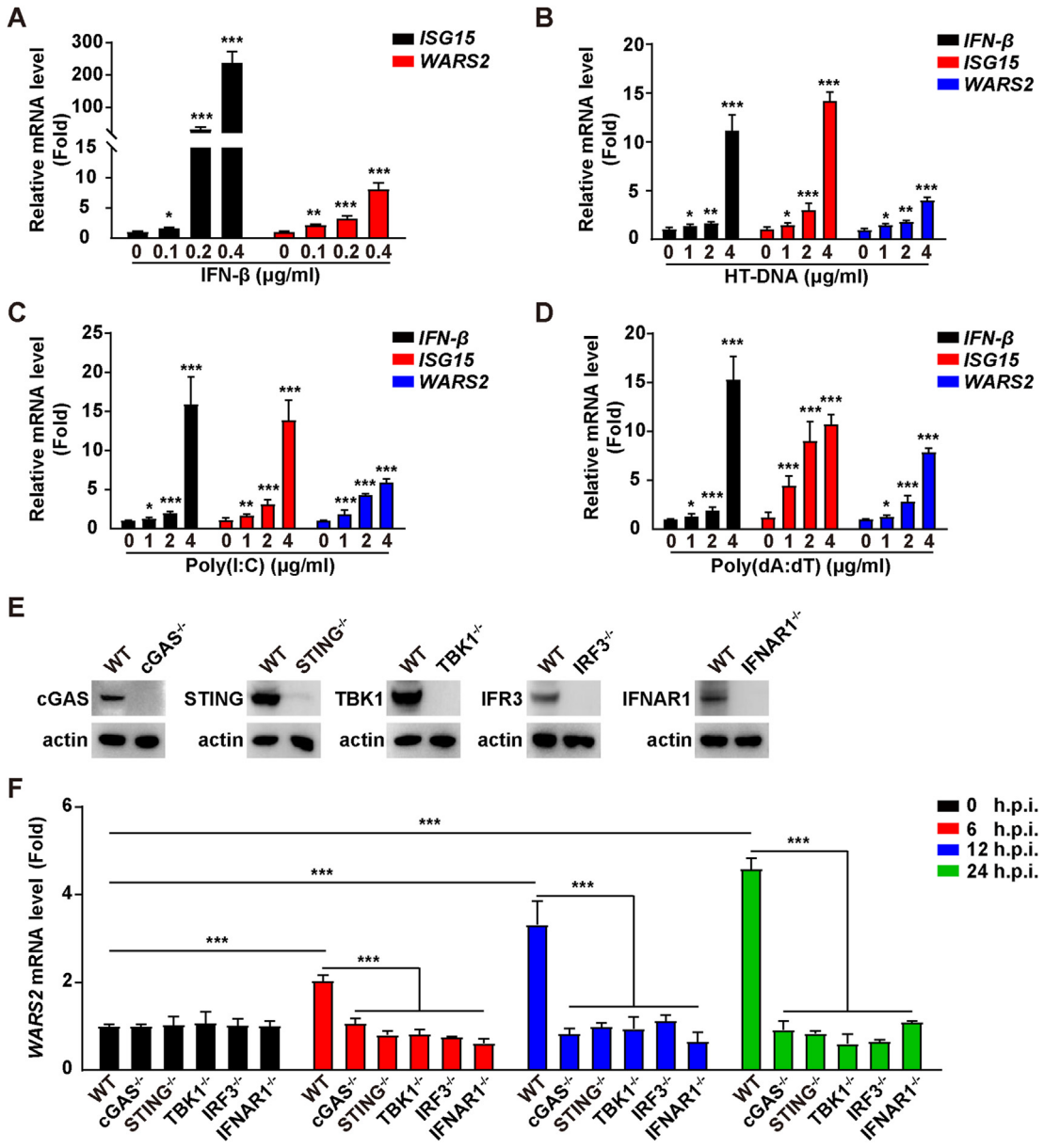

Fig. 2. WARS2 expression is dependent on type I IFN and cGAS-mediated innate immune pathway. **A** PK-15 cells were exposed to IFN-β (0–0.4 μg/mL) for 24 h. qRT-PCR analysis was employed to determine the expression levels of ISG15 and WARS2 mRNA. $^{*}P < 0.05$, $^{**}P < 0.01$, $^{***}P < 0.001$. **B–D** PK-15 cells underwent transfection with varying concentrations of HT-DNA (0–4 μg/mL) (**B**), poly (I:C) (0–4 μg/mL) (**C**), and poly (dA:dT) (0–4 μg/mL) (**D**) for 2 h. qRT-PCR analysis was conducted to quantify the mRNA expression levels of IFN-β, ISG15, and WARS2. $^{*}P < 0.05$, $^{**}P < 0.01$, $^{***}P < 0.001$. **E** The presence of cGAS, STING, TBK1, IRF3, and IFNAR1 proteins was analyzed through immunoblotting analysis in *cGAS*$^{-/-}$, *STING*$^{-/-}$, *TBK1*$^{-/-}$, *IRF3*$^{-/-}$ and *IFNAR1*$^{-/-}$ PK-15 cells. **F** *cGAS*$^{-/-}$, *STING*$^{-/-}$, *TBK1*$^{-/-}$, *IRF3*$^{-/-}$ and *IFNAR1*$^{-/-}$ PK-15 cells were subjected to infection with PRV-QXX at a MOI of 1 for 0–24 h. The expression level of WARS2 mRNA in these cells was quantified using qRT-PCR analysis. $^{***}P < 0.001$.

chase assay was employed. Puromycin integrates into nascent polypeptide chains, enabling detection via immunoblotting with a puromycin-specific antibody. Compared to mock-infected conditions, puromycin labeling of proteins was markedly intensified post-PRV infection, whereas WARS2 knockdown resulted in attenuated protein synthesis (Fig. 5B). The eukaryotic initiation factor 2 alpha (eIF2α) can promote the recruitment of Met-tRNAi to 40S/mRNA complexes under conditions of inhibition of eIF2 activity (via eIF2α phosphorylation). Being a pivotal translation initiation regulator, eIF2α's phosphorylation status at Ser51 significantly influences global translation rates (Desmet et al., 2014). As shown in Fig. 5B, phosphorylated eIF2α levels were diminished in PRV-infected cells but were notably reduced to near indetectability in scramble cells. Conversely, WARS2 silencing manifests a substantial elevation in p-eIF2α levels. Meanwhile, overexpression of WARS2 enhanced protein synthesis (Fig. 5C).

To further probe the functional significance of WARS2 in the propagation of PRV, rescue assays were performed by transfecting shWARS2-1-depleted PK-15 cells with either an expression vector encoding a WARS2 variant with a mutation compromising its enzymatic function, FLAG-WARS2 mut (48–54) (Antonellis and Green, 2008; Wang et al., 2016), or an expression vector lacking the mitochondrial targeting sequence, FLAG-WARS2 Δ(1–18) (Martinelli et al., 2020). Assessment through both immunoblotting and viral titration methodologies revealed that reintroduction of wild-type FLAG-WARS2 restored both protein biosynthesis and PRV replication. In contrast, cells transfected with either of the mutant WARS2 constructs did not exhibit such rescue effects (Fig. 5D and E). These results suggest that the depletion of WARS2 impedes PRV-mediated protein synthesis.

Given the role of WARS2 as an mtARS, potentially implicated in the modulation of mitochondrial oxidative phosphorylation, an investigation was initiated to discern its effects on the protein constituents of

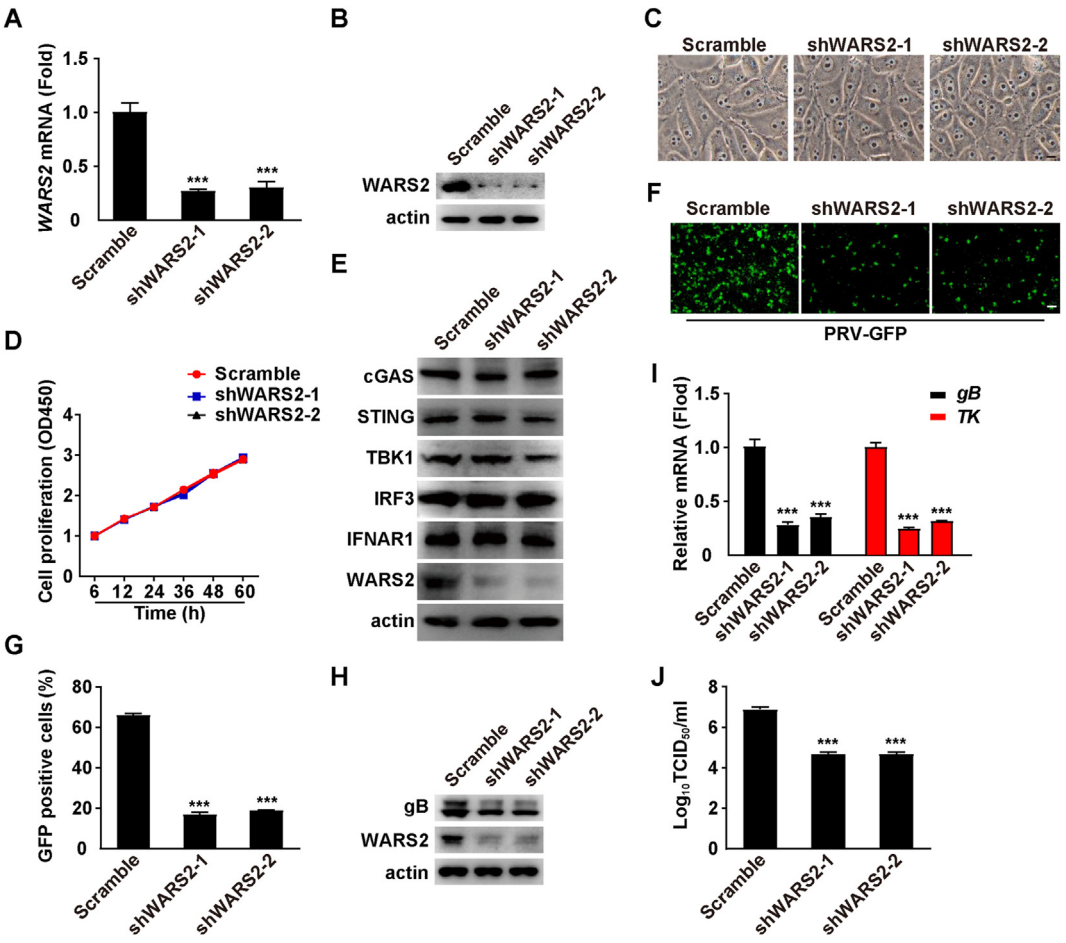

Fig. 3. Suppression of WARS2 attenuates PRV infection. **A** WARS2 mRNA expression was quantitatively measured in scramble, shWARS2-1, and shWARS2-2 PK-15 cells using qRT-PCR analysis. $^{***}P < 0.001$. **B** Protein levels of WARS2 in PK-15 cells treated as described in **A** were determined via immunoblotting analysis. **C** Comparative morphology of PK-15 cells treated as in **A** was documented. Scale bar, 10 μm. **D** The viability of PK-15 cells with different WARS2 expression levels was evaluated over a time course of 0–60 h using a CCK-8 assay. **E** Protein levels of cGAS, STING, TBK1, IRF3, IFNAR1 and WARS2 were assessed by immunoblotting analysis in scramble, shWARS2-1, and shWARS2-2 PK-15 cells. **F** PK-15 cells, treated as mentioned above, were infected with PRV-GFP at an MOI of 1 for 20 h. GFP expression, indicative of viral replication, was monitored through fluorescence microscopy. Scale bar, 100 μm. **G** GFP-positive cells from the experiment in **F** were quantitated by flow cytometry. $^{***}P < 0.001$. **H** WARS2 and PRV gB levels were assessed by immunoblotting analysis in scramble, shWARS2-1, and shWARS2-2 PK-15 cells infected with PRV-QXX at an MOI of 1 for 24 h. **I** qRT-PCR analysis was employed to quantify PRV gB and TK mRNA expression in scramble, shWARS2-1, and shWARS2-2 PK-15 cells infected with PRV-QXX at an MOI of 1 for 24 h. $^{***}P < 0.001$. **J** Viral titers in samples from **H** were determined via a $TCID_{50}$ assay. $^{***}P < 0.001$.

mitochondrial oxidative phosphorylation complexes. To this end, both control and WARS2-deficient cells were infected with PRV-QXX, followed by the quantification of protein levels of essential components of the mitochondrial oxidative phosphorylation pathway, comprising Complex I (NDUFA9), Complex II (SDHA), and Complex IV (COX1). Immunoblotting analyses revealed an upregulation in the expressions of NDUFA9, SDHA, and COX1 consequential to PRV infection (Fig. 5F). Conversely, the ablation of WARS2 negated the PRV elicited enhancements in these oxidative phosphorylation complex components (Fig. 5F). These findings intimate that WARS2 depletion mitigates the oxidative phosphorylation activation triggered by PRV, potentially culminating in diminished mitochondrial respiration and compromised ATP production. Given the pivotal role of ATP as the chief cellular energy reservoir and acetyl-CoA as a critical metabolic intermediary, additional explorations were undertaken to ascertain WARS2's influence on cellular metabolism, through measurements of ATP and acetyl-CoA concentrations in control and WARS2-depleted cells, post-PRV-QXX infection, across a temporal window of 0–24 h. PRV infection elicited an augmentation in intracellular ATP concentrations (Fig. 5G), whereas WARS2 suppression did not significantly alter ATP levels (Fig. 5G). Analogously, acetyl-CoA quantities increased after PRV infection, with no significant variation observed following WARS2 knockdown (Fig. 5H). Cumulatively, these data substantiate the essentiality of WARS2 in fostering PRV-driven protein biosynthesis, cellular oxidative phosphorylation, and the biosynthesis of ATP and acetyl-CoA.

3.6. *WARS2 knockdown reduces PRV-induced lipid synthesis*

Acetyl-CoA plays a central role in various metabolic pathways, notably in the biosynthesis of fatty acids, a process predominantly located in the cytoplasm and characterized by its high demand for ATP. Our prior research identified that the downregulation of WARS2 alters cellular ATP and acetyl-CoA concentrations. Consequently, the implication of WARS2 in lipid metabolic pathways was further explored. Initial assessments involved quantifying the lipid droplet (LD) accumulation within a temporal framework of 0–24 h post-infection in both control (scramble) and WARS2-deficient cells exposed to PRV-QXX. Employing Oil red O staining, it was observed that PRV infection enhances LD formation in scramble cells, an effect that was not replicated in cells lacking WARS2 (Fig. 6A and B). We further quantified the impact on intracellular lipid profiles, indicating elevations in total cholesterol (TC), triglycerides (TG), and free fatty acids (FFAs) following PRV infection in scramble

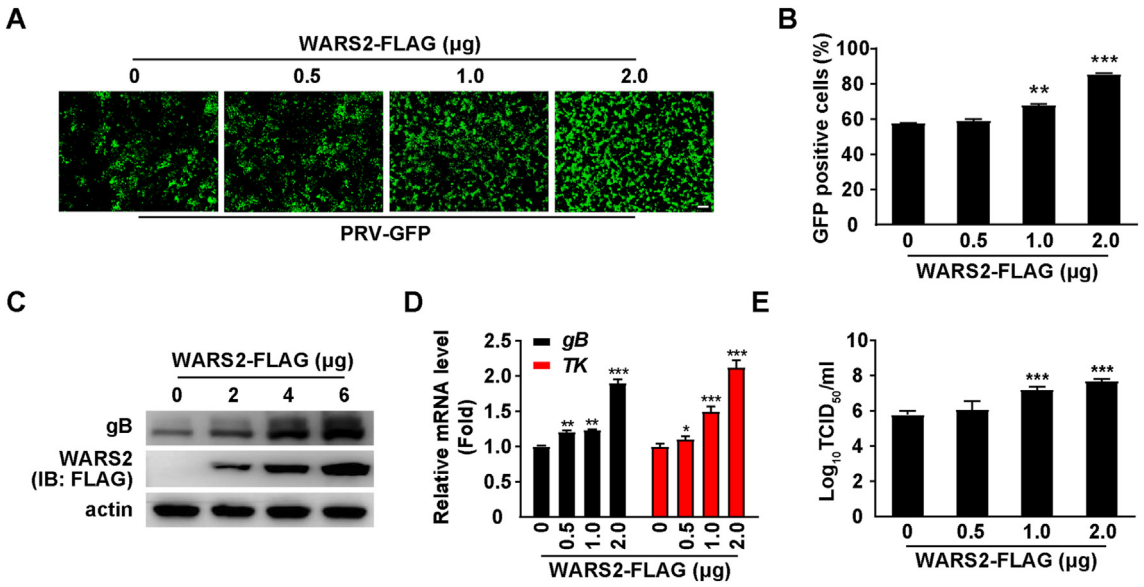

Fig. 4. Enhancement of PRV infection through WARS2 overexpression. **A** PK-15 cells, post-transfection with FLAG-WARS2 plasmid (0–2 μg) for 12 h, were infected with PRV-GFP at a MOI of 1 for 20 h. GFP expression, as a marker of viral replication, was visualized using fluorescence microscopy. Scale bar, 100 μm. **B** Quantification of GFP-positive cells from **A** via flow cytometry. $^{**}P < 0.01$, $^{***}P < 0.001$. **C** Following a similar procedure as in **A** but with varying plasmid concentrations (0–6 μg), PRV gB and WARS2-FLAG protein levels were evaluated using immunoblotting analysis. **D** qRT-PCR analysis was utilized to assess PRV gB and TK mRNA levels in PK-15 cells transfected with the FLAG-WARS2 plasmid (0–2 μg) for 12 h and then infected with PRV-QXX at a MOI of 1 for 24 h. $^{*}P < 0.05$, $^{**}P < 0.01$, $^{***}P < 0.001$. **E** Viral replication in PK-15 cells treated as in **D** was determined via a $TCID_{50}$ assay. $^{***}P < 0.001$.

cells. In contrast, the abrogation of WARS2 negated this lipid accumulation, underscoring the pivotal necessity of WARS2 for lipid biosynthesis (Fig. 6C–E). This accords with previous observations suggesting that the inhibition of LD biogenesis negatively influences PRV replication (Li et al., 2023), whereby WARS2 depletion compromised the PRV-induced augmentation in LD numbers and lipid accumulation.

To elucidate the impact of WARS2 downregulation on lipid biosynthesis, cells subjected to RNAi targeting WARS2 and respective controls were infected with PRV-QXX. The investigation focused on the transcriptional levels of pivotal lipid biosynthesis regulators, including sterol regulatory element-binding protein 1c (SREBP1c), fatty acid synthase (FASN), acetyl-CoA carboxylase alpha (ACACA), sterol regulatory element-binding protein 2 (SREBP2), and 3-hydroxy-3-methylglutaryl-CoA reductase (HMGCR). Quantitative reverse transcription PCR (qRT-PCR) analyses demonstrated an absence of PRV-induced mRNA augmentation for these regulatory factors in cells with WARS2 knockdown, in comparison to control groups (Fig. 6F–J). Furthermore, immunoblotting assays indicated that PRV infection resulted in the upregulation of ACACA, HMGCR, and FASN expression (Fig. 6K). However, this upregulation was mitigated in the presence of WARS2 knockdown (Fig. 6K). Additionally, an elevated phosphorylation state of HMGCR and ACACA was detected in WARS2-deficient PK-15 cells, indicating potential inactivation of these enzymes consequent to WARS2 silencing (Fig. 6K), a process known to render HMGCR and ACACA enzymatically inactive upon phosphorylation (Day et al., 2021). To validate these outcomes, a rescue assay incorporating oleic acid (OA) was conducted, wherein the incorporation of OA into the media of WARS2-deficient cells correlated with increased PRV titers, as measured by $TCID_{50}$ assay, contingent on OA concentration increments (Fig. 6L). We further quantified the impact of WARS2 overexpression on intracellular lipid profiles, indicating elevations in TC, TG, and FFAs (Fig. 6M–O). Collectively, these findings highlight the essential contribution of WARS2 to PRV-enhanced lipid biosynthesis.

4. Discussion

Viruses function as obligate intracellular parasites, necessitating host cellular machinery for their propagation (Wang and Li, 2012). The interaction in nutrient metabolism between host organisms and viruses provides insights into the pathogenesis of a myriad of viral-induced infectious diseases. This knowledge is instrumental in identifying viable targets for antiviral therapeutic development, particularly because the modulation of host factors introduces a substantial genetic hurdle that could inhibit the evolution of viral resistance mechanisms (Wang and Li, 2012; Allen et al., 2022). The metabolic pathways concerning proteins and lipids within host cells are critical for viral replication processes (Lorizate and Krausslich, 2011; Allen et al., 2022), However, the role of these metabolic pathways in the replication of PRV remains inadequately explored. Within the scope of the present research, it has been evidenced that PRV infection facilitates the amplification of both protein and lipid biosynthesis, which is mediated by an upsurge in WARS2 expression. This upregulation is attributed to the activation of cGAS/STING innate immune response and IFN signaling pathways (Fig. 7).

The innate immune system has evolved to serve as a primary defense mechanism against viral infections. The DNA-dependent activator of IFN-regulatory factors has been identified as an essential sensor for the detection of viral DNA, initiating the immune response to viral invasion (Takaoka et al., 2007; Wang et al., 2007). The detection of cytoplasmic DNA by these molecular sensors represents a critical juncture in the innate immune response to viral infection, instigating the synthesis of type I interferon, cytokines, and chemokines. These constituents significantly contribute to the antiviral defense, being generated via cascading amplification reactions that bolster the innate antiviral response (Keating et al., 2011). However, not all ISGs possess the capacity to counteract viral infection. Previous research has indicated that the transmembrane protein 41B, classified as an ISG, facilitates the replication of PRV (Li et al., 2023). It has been documented that the innate immune machinery, upon PRV infection, initiates a response mediated by cytosolic pattern recognition receptors that detect PRV genomic DNA (Xie et al., 2010; Li et al., 2023). Nevertheless, investigations remain to conclusively determine the involvement of these DNA sensors in influencing WARS2 expression. Historical evidence from 1991 revealed a protein, highly inducible by IFN-gamma, known as protein g2, to be identical to the human cytoplasmic WARS (Bonnevie-Nielsen et al., 1991; Fleckner et al., 1991; Frolova et al., 1993). Subsequent research has elucidated the association between WARS expression and immune modulation, alongside

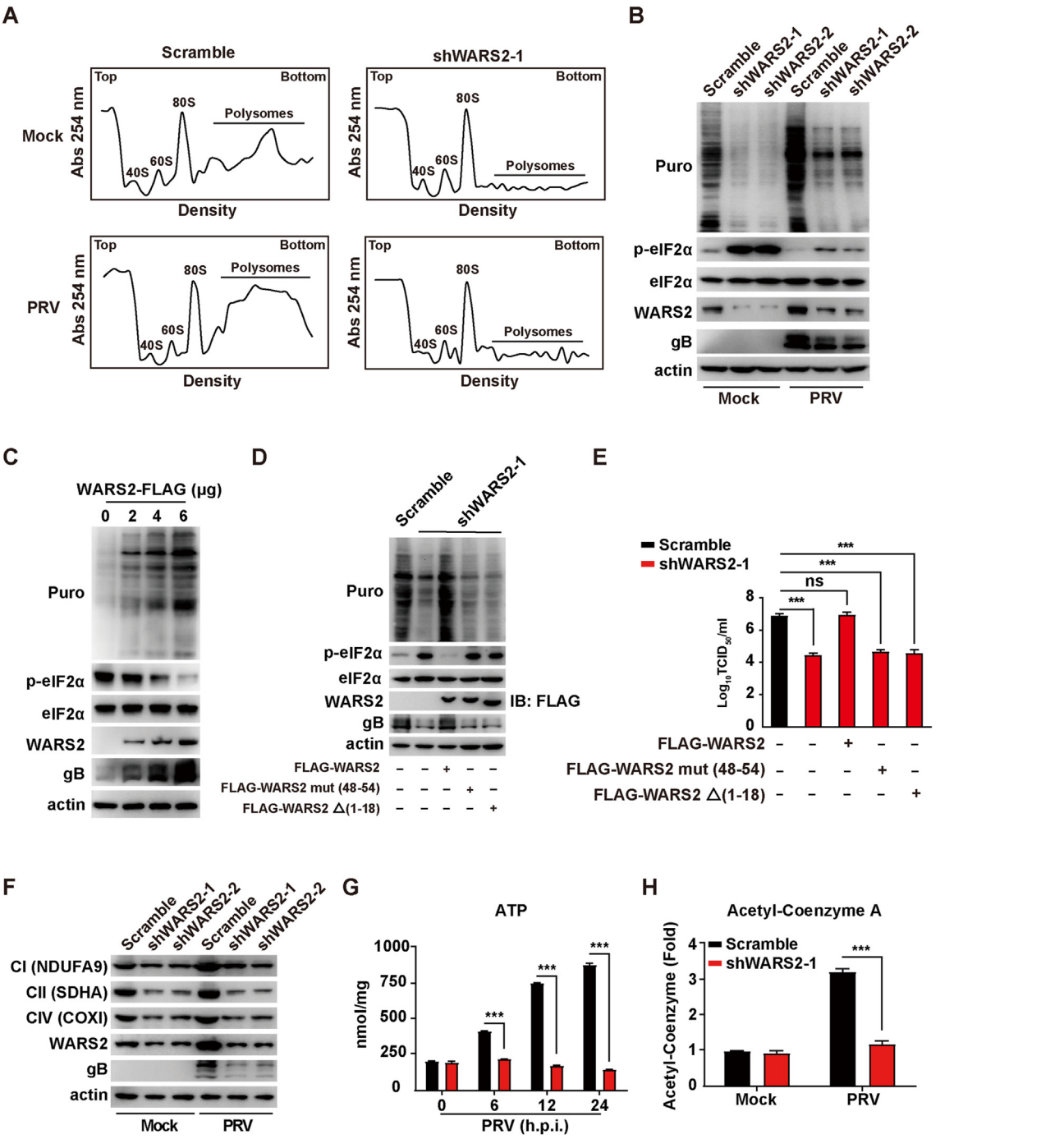

Fig. 5. Contribution of WARS2 to protein, ATP, and acetyl-CoA synthesis. **A** Scramble and shWARS2-1 PK-15 cells were infected with PRV-QXX at a MOI of 1 for 24 h. The optical density was measured at a wavelength of 254 nm (OD_{254}) with varioskan flash. **B** Scramble, shWARS2-1 and shWARS2-2 PK-15 cells were mock-infected or infected with PRV-QXX at a MOI of 1 for 24 h, and then pulsed with 5 μg/mL puro for 15 min. Puro, p-eIF2α, eIF2α, WARS2 and PRV gB were assessed by immunoblotting analysis. **C** PK-15 cells were transfected with WARS2-FLAG (0–6 μg) for 24 h, and then pulsed with 5 μg/mL puro for 15 min. Puro, p-eIF2α, eIF2α, WARS2 and PRV gB were assessed by immunoblotting analysis. **D** Scramble and shWARS2-1 PK-15 cells were transfected with the FLAG-WARS2, FLAG-WARS2 mut (48–54) and FLAG-WARS2 Δ(1–18) plasmid 6 μg for 12 h, and infected with PRV-QXX at a MOI of 1 for 24 h. Puro, p-eIF2α, eIF2α, WARS2-FLAG and PRV gB were assessed by immunoblotting analysis. **E** Cells were infected and treated as in **D**. Viral titers were assessed by a $TCID_{50}$ assay. $^{***}P < 0.001$. ns, no significance. **F** Scramble, shWARS2-1 and shWARS2-2 PK-15 cells were mock-infected or infected with PRV-QXX at a MOI of 1 for 24 h. NDUFA9 (CI), SDHA (CII), COX1 (CIV), WARS2 and gB were assessed by immunoblotting analysis. **G** Scramble and shWARS2-1 PK-15 cells were infected with PRV-QXX at a MOI of 1 for 0–24 h. Cellular ATP was quantified using biochemical kits. $^{***}P < 0.001$. **H** Scramble and shWARS2-1 PK-15 cells were infected with PRV-QXX at a MOI of 1 for 24 h. Cellular acetyl-CoA was quantified using biochemical kits. $^{***}P < 0.001$.

its correlation with favorable tumor prognosis (Lu et al., 2020). Given the significant role of WARS in immune regulation, its relevance in the context of viral infections is substantial. Prior investigations have illuminated the critical function of WARS in facilitating the entry and infection of enteroviruses (Yeung et al., 2018; Masomian et al., 2021). Moreover, it has been shown that WARS is swiftly secreted following viral infection, initiating the innate immune response through the induction of proinflammatory cytokines and type I IFN secretion (Lee et al.,

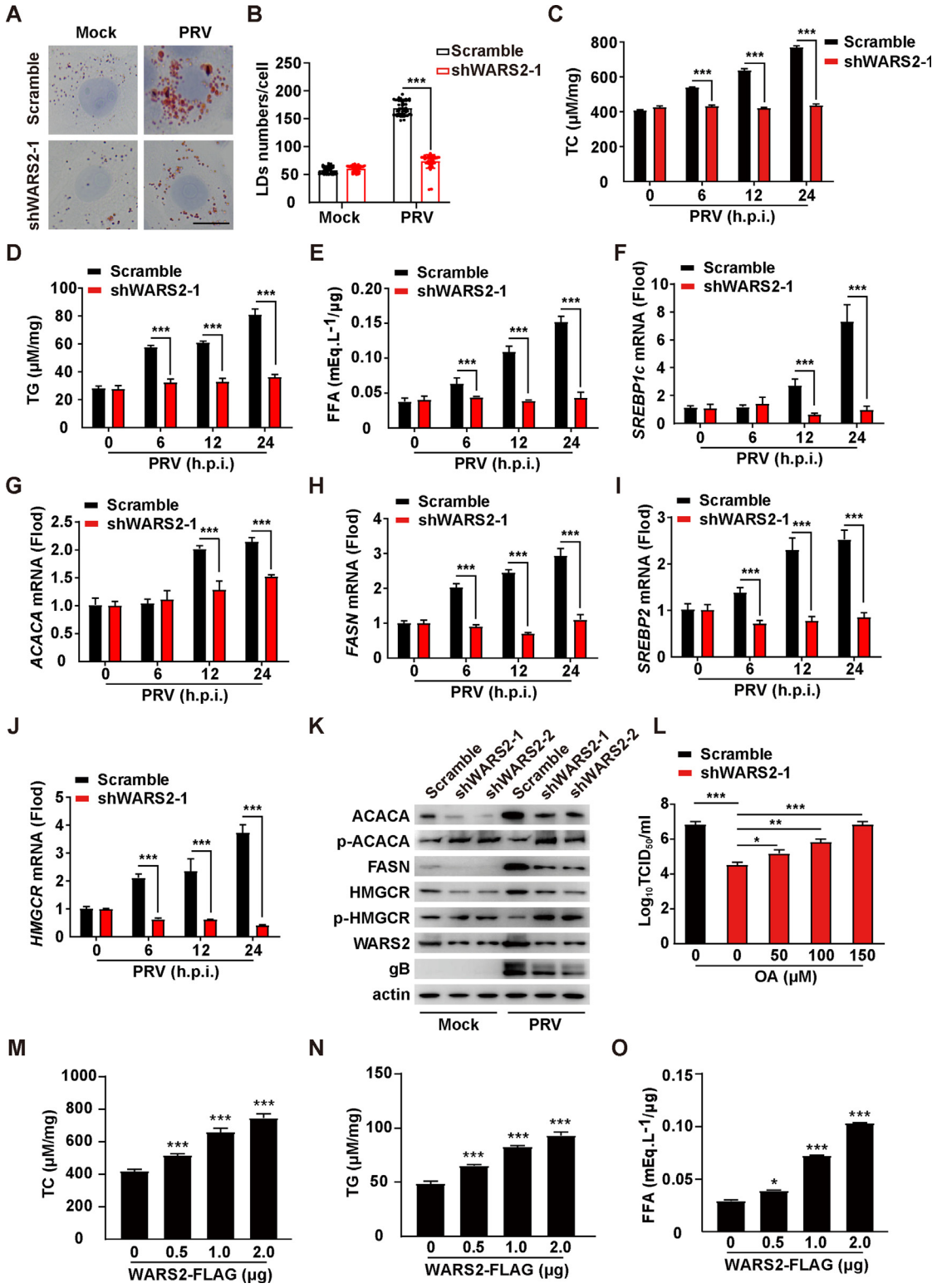

Fig. 6. WARS2's role in PRV-induced lipid synthesis. **A** LDs were visualized in scramble and shWARS2-1 PK-15 cells post-infection with PRV-QXX at a MOI of 1 for 24 h using Oil Red O staining. Scale bar, 10 μm. **B** LDs quantification per cell from **A** was performed using ImageJ analysis (n = 50). ***$P < 0.001$. **C–E** Quantification of TC (**C**), TG (**D**), and FFAs (**E**) in scramble and shWARS2-1 PK-15 cells was accomplished using biochemical kits following infection with PRV-QXX at a MOI of 1 for 0–24 h. ***$P < 0.001$. **F–J** mRNA expression levels of SREBP1c (**F**), ACACA (**G**), FASN (**H**), SREBP2 (**I**), and HMGCR (**J**) in scramble, shWARS2-1, and shWARS2-2 PK-15 cells were measured via qRT-PCR analysis. ***$P < 0.001$. **K** The expression of lipid metabolism enzymes and viral proteins in scramble, shWARS2-1, and shWARS2-2 PK-15 cells mock-infected or infected with PRV-QXX at a MOI of 1 for 24 h were assessed by immunoblotting analysis. **L** Viral titers in scramble and shWARS2-1 PK-15 cells, infected with PRV-QXX at a MOI of 1 and treated with oleic acid (OA at 150 μM) for 24 h, were determined through a $TCID_{50}$ assay. *$P < 0.05$, **$P < 0.01$, ***$P < 0.001$. **M–O** Quantification of TC (**F**), TG (**G**), and FFAs (**H**) in WARS2-FLAG (0–2 μg) transfected PK-15 cells was accomplished using biochemical kits. *$P < 0.05$, ***$P < 0.001$.

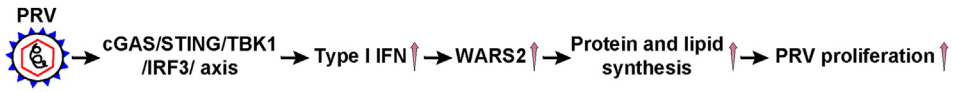

Fig. 7. Schematic model of PRV manipulates mitochondrial tryptophanyl-tRNA synthetase 2 for viral replication. PRV infection activates the cGAS/STING/TBK1/IRF3 innate immune pathway, mediating type I interferon production, which in turn stimulates WARS2 expression. This enhancement in WARS2 activity boosts protein and lipid synthesis, facilitating subsequent viral replication.

2019). Recent studies have underscored the supportive role of WARS in augmenting innate immunity against coronavirus disease 2019 (Maras et al., 2021; Najimi et al., 2023). Despite the limited research available on the role of WARS in viral infections, this study delineates how PRV infection mediates the upregulation of WARS2 expression via the IFN signaling pathway.

Owing to the lack of genes encoding for mRNA translation machinery, viruses universally exploit host cellular ribosomes for the synthesis of viral proteins (Cao et al., 2017). Many viruses induce a widespread suppression of host protein production, a process termed as "host shutoff" (Gale et al., 2000; Walsh and Mohr, 2011). Nevertheless, infections caused by the PRV have been documented to provoke an enhancement in the host's protein synthesis (Zhu et al., 2021). ARS are pivotal enzymes within the translational apparatus, facilitating the linkage of specific amino acids to their respective tRNA molecules, thereby playing an indispensable role in protein biosynthesis in host cells (Yao and Fox, 2013). In parallel, lipid metabolism is crucial for viral replication, serving as an energy reservoir for the replication processes of viruses (Allen et al., 2022). Previous investigations have demonstrated that epigallocatechin gallate can impede the replication and assembly of the porcine reproductive and respiratory syndrome virus by interrupting lipid metabolic pathways (Yu et al., 2022). Moreover, lipid metabolic processes, influenced by Niemann-Pick type C1, Liver X receptor, and transmembrane protein 41B, have been found to modulate the entry mechanism of PRV into host cells (Li et al., 2022, 2023; Wang et al., 2022). There is a significant correlation between lipid metabolism and the innate immune defense against viral infections (Xiao et al., 2020). For instance, cholesterol-25-hydroxylase is capable of obstructing viral entry and exerting a wide range of antiviral effects through the biosynthesis of 25-hydroxycholesterol (Liu et al., 2013; Wang et al., 2017). Additionally, the role of 7-dehydrocholesterol in modulating the production of type I IFN via the activation of AKT serine/threonine kinase 3, which leads to diverse antiviral outcomes, has been documented (Xiao et al., 2020). Our investigation has elucidated that WARS2 facilitates PRV infection, revealing a previously unidentified mechanism through which an interferon-stimulated gene may enhance viral replication. Moreover, our findings further delineate the integral roles of WARS2 in promoting PRV-induced protein and lipid biosynthesis. Innate immunity is indispensable for the organism's defense against pathogens and is increasingly recognized for its regulatory influence on various physiological processes, including lipid metabolism. Activation of innate immune pathways precipitates the secretion of cytokines, such as tumor necrosis factor-alpha, interleukins, and interferons, which can modulate lipid metabolism through various mechanisms, including the alteration of lipoprotein concentrations, the modification of enzymatic activities related to lipid biosynthesis and degradation, and the impact on lipid storage within adipocytes (Chen et al., 2019).

5. Conclusions

The results of this study elucidate that WARS2 is integral in promoting PRV replication within the host organism. This observation proposes the inhibition of WARS2 as a potential strategy for the formulation of pharmacological agents and vaccinations aimed at curtailing the replication of PRV. Through the targeted inhibition of WARS2, there exists the potential to mitigate the dissemination and intensity of PRV infections. Consequently, these findings offer significant insights and establish a foundation for subsequent explorations aimed at the identification and development of efficacious therapeutic interventions against PRV.

Data availability

All the data generated during the current study are included in the manuscript.

Ethics statement

Experiments involving animals were approved by the Committee on the Ethics of Animal Care and Use of Henan Agricultural University (HNND2019031004). The study was conducted in accordance with the Guide for the Care and Use of Animals in Research of the People's Republic of China.

Author contributions

Xiu-Qing Li, Meng-Pan Cai: formal analysis, investigation, methodology, validation, visualization. Bei-Bei Chu, Jiang Wang: funding acquisition, conceptualization, supervision, project administration, writing-original draft, writing-review & editing. Sheng-Li Ming: conceptualization, supervision, project administration. Ming-Yang Wang: data curation, software, validation, visualization. Guo-Yu Yang: data curation, funding acquisition, visualization.

Conflict of interest

The authors declare that they have no competing interests.

Acknowledgements

This research is supported by grants from the National Key R&D Program of China (2023YFD1801600 and 2021YFD1301200), and Henan Province Higher Education Teaching Reform Research and Practice Project (2021SJGLX351).

Appendix A. Supplementary data

Supplementary data to this article can be found online at https://doi.org/10.1016/j.virs.2024.04.003.

References

Ai, J.W., Weng, S.S., Cheng, Q., Cui, P., Li, Y.J., Wu, H.L., Zhu, Y.M., Xu, B., Zhang, W.H., 2018. Human endophthalmitis caused by pseudorabies virus infection, China, 2017. Emerg. Infect. Dis. 24, 1087–1090.

Allen, C., Arjona, S., Santerre, M., Sawaya, B., 2022. Hallmarks of metabolic reprogramming and their role in viral pathogenesis. Viruses 14, 602.

Antonellis, A., Green, E., 2008. The role of aminoacyl-tRNA synthetases in genetic diseases. Annu. Rev. Genomics Hum. Genet. 9, 87–107.

Bonnevie-Nielsen, V., Gerdes, A., Fleckner, J., Petersen, J., Michelsen, B., Dyrberg, T., 1991. Interferon stimulates the expression of 2',5'-oligoadenylate synthetase and MHC class I antigens in insulin-producing cells. J. Interferon Res. 11, 255–260.

Burke, E., Frucht, S., Thompson, K., Wolfe, L., Yokoyama, T., Bertoni, M., Huang, Y., Sincan, M., Adams, D., Taylor, R., Gahl, W., Toro, C., Malicdan, M., 2018. Biallelic mutations in mitochondrial tryptophanyl-tRNA synthetase cause Levodopa-responsive infantile-onset Parkinsonism. Clin. Genet. 93, 712–718.

Cao, S., Dhungel, P., Yang, Z., 2017. Going against the tide: selective cellular protein synthesis during virally induced host shutoff. J. Virol. 91, e00071-17.

Chen, Y., Yu, C.Y., Deng, W.M., 2019. The role of pro-inflammatory cytokines in lipid metabolism of metabolic diseases. Int. Rev. Immunol. 38, 249–266.

Curtis, C., Shah, S., Chin, S., Turashvili, G., Rueda, O., Dunning, M., Speed, D., Lynch, A., Samarajiwa, S., Yuan, Y., Gräf, S., Ha, G., Haffari, G., Bashashati, A., Russell, R., Mckinney, S., Langerød, A., Green, A., Provenzano, E., Wishart, G., Pinder, S., Watson, P., Markowetz, F., Murphy, L., Ellis, I., Purushotham, A., Børresen-Dale, A., Brenton, J., Tavaré, S., Caldas, C., Aparicio, S., 2012. The genomic and transcriptomic architecture of 2,000 breast tumours reveals novel subgroups. Nature 486, 346–352.

Day, E., Ford, R., Smith, B., Houde, V., Stypa, S., Rehal, S., Lhotak, S., Kemp, B., Trigatti, B., Werstuck, G., Austin, R., Fullerton, M., Steinberg, G., 2021. Salsalate reduces atherosclerosis through AMPKβ1 in mice. Mol. Metab. 53, 101321.

Desmet, E.A., Anguish, L.J., Parker, J.S., 2014. Virus-mediated compartmentalization of the host translational machinery. mBio 5, e01463-01414.

Fleckner, J., Rasmussen, H., Justesen, J., 1991. Human interferon gamma potently induces the synthesis of a 55-kDa protein (gamma 2) highly homologous to rabbit peptide chain release factor and bovine tryptophanyl-tRNA synthetase. Proc. Natl. Acad. Sci. U. S. A. 88, 11520–11524.

Frolova, Lyu, Fleckner, J., Justesen, J., Timms, K., Tate, W., Kisselev, L., Haenni, A., 1993. Are the tryptophanyl-tRNA synthetase and the peptide-chain-release factor from higher eukaryotes one and the same protein? Eur. J. Biochem. 212, 457–466.

Gack, M.U., Wang, J., Li, G.-L., Ming, S.-L., Wang, C.-F., Shi, L.-J., Su, B.-Q., Wu, H.-T., Zeng, L., Han, Y.-Q., Liu, Z.-H., Jiang, D.-W., Du, Y.-K., Li, X.-D., Zhang, G.-P., Yang, G.-Y., Chu, B.-B., 2020. BRD4 inhibition exerts anti-viral activity through DNA damage-dependent innate immune responses. PLoS Pathog. 16, e1008429.

Gale, M., Tan, S., Katze, M., 2000. Translational control of viral gene expression in eukaryotes. Microbiol. Mol. Biol. Rev. 64, 239–280.

Han, S., Sun, S., Li, P., Liu, Q., Zhang, Z., Dong, H., Sun, M., Wu, W., Wang, X., Guo, H., 2020. Ribosomal protein L13 promotes IRES-driven translation of foot-and-mouth disease virus in a helicase DDX3-dependent manner. J. Virol. 94, e01679–19.

Heid, I., Jackson, A., Randall, J., Winkler, T., Qi, L., Steinthorsdottir, V., Thorleifsson, G., Zillikens, M., Speliotes, E., Mägi, R., et al., 2010. Meta-analysis identifies 13 new loci associated with waist-hip ratio and reveals sexual dimorphism in the genetic basis of fat distribution. Nat. Genet. 42, 949–960.

Keating, S.E., Baran, M., Bowie, A.G., 2011. Cytosolic DNA sensors regulating type I interferon induction. Trends Immunol. 32, 574–581.

Lee, H., Lee, E., Uddin, M., Kim, T., Kim, J., Chathuranga, K., Chathuranga, W., Jin, M., Kim, S., Kim, C., Lee, J., 2019. Released tryptophanyl-tRNA synthetase stimulates innate immune responses against viral infection. J. Virol. 93, e01291-18.

Li, G., Su, B., Fu, P., Bai, Y., Ding, G., Li, D., Wang, J., Yang, G., Chu, B., 2022. NPC1-regulated dynamic of clathrin-coated pits is essential for viral entry. Sci. China Life Sci. 65, 341–361.

Li, X., Zeng, L., Liang, D., Qi, Y., Yang, G., Zhong, K., Chu, B., Wang, J., 2023. TMEM41B is an interferon-stimulated gene that promotes pseudorabies virus replication. J. Virol. 93, e0041223.

Li, Y., Chang, H., Yang, X., Zhao, Y., Chen, L., Wang, X., Liu, H., Wang, C., Zhao, J., 2015. Antiviral activity of porcine interferon regulatory factor 1 against swine viruses in cell culture. Viruses 7, 5908–5918.

Liu, F., Smith, J., Zhang, Z., Cole, R., Herron, B., 2010. Genetic heterogeneity of skin microvasculature. Dev. Biol. 340, 480–489.

Liu, S.Y., Aliyari, R., Chikere, K., Li, G., Marsden, M.D., Smith, J.K., Pernet, O., Guo, H., Nusbaum, R., Zack, J.A., Freiberg, A.N., Su, L., Lee, B., Cheng, G., 2013. Interferon-inducible cholesterol-25-hydroxylase broadly inhibits viral entry by production of 25-hydroxycholesterol. Immunity 38, 92–105.

Lorizate, M., Krausslich, H.G., 2011. Role of lipids in virus replication. Cold Spring Harb. Perspect. Biol. 3, a004820.

Lu, S., Wang, L., Lombardo, K., Kwak, Y., Kim, W., Resnick, M., 2020. Expression of indoleamine 2, 3-dioxygenase 1 (IDO1) and tryptophanyl-tRNA synthetase (WARS) in gastric cancer molecular subtypes. Appl. Immunohistochem. Mol. Morphol. 28, 360–368.

Maras, J., Sharma, S., Bhat, A., Rooge, S., Aggrawal, R., Gupta, E., Sarin, S., 2021. Multi-omics analysis of respiratory specimen characterizes baseline molecular determinants associated with SARS-CoV-2 outcome. iScience 24, 102823.

Martinelli, S., Cordeddu, V., Galosi, S., Lanzo, A., Palma, E., Pannone, L., Ciolfi, A., Di Nottia, M., Rizza, T., Bocchinfuso, G., et al., 2020. Co-occurring WARS2 and CHRNA6 mutations in a child with a severe form of infantile parkinsonism. Parkinsonism Relat. Disord. 72, 75–79.

Masomian, M., Lalani, S., Poh, C., 2021. Molecular docking of SP40 peptide towards cellular receptors for Enterovirus 71 (EV-A71). Molecules 26, 6576.

Mettenleiter, T.C., 1999. Aujeszky's disease (pseudorabies) virus: the virus and molecular pathogenesis. Vet. Res. 31, 99–115.

Najimi, N., Zahednasab, H., Farahmand, M., Fouladvand, A., Talei, G., Bouzari, B., Khanizadeh, S., Karampoor, S., 2023. Exploring the role of tryptophanyl-tRNA synthetase and associations with inflammatory markers and clinical outcomes in COVID-19 patients: a case-control study. Microb. Pathog. 183, 106300.

Pomeranz, L.E., Reynolds, A.E., Hengartner, C.J., 2005. Molecular biology of pseudorabies virus: impact on neurovirology and veterinary medicine. Microbiol. Mol. Biol. Rev. 69, 462–500.

Sánchez, E., Quintas, A., Nogal, M., Castelló, A., Revilla, Y., 2013. African swine fever virus controls the host transcription and cellular machinery of protein synthesis. Virus Res. 173, 58–75.

Skorvanek, M., Rektorova, I., Mandemakers, W., Wagner, M., Steinfeld, R., Orec, L., Han, V., Pavelekova, P., Lackova, A., Kulcsarova, K., Ostrozovicova, M., Gdovinova, Z., Plecko, B., Brunet, T., Berutti, R., Kuipers, D., Boumeester, V., Havrankova, P., Tijssen, M., Kaiyrzhanov, R., Rizig, M., Houlden, H., Winkelmann, J., Bonifati, V., Zech, M., Jech, R., 2022. WARS2 mutations cause dopa-responsive early-onset parkinsonism and progressive myoclonus ataxia. Parkinsonism Relat. Disord. 94, 54–61.

Takaoka, A., Wang, Z., Choi, M.K., Yanai, H., Negishi, H., Ban, T., Lu, Y., Miyagishi, M., Kodama, T., Honda, K., Ohba, Y., Taniguchi, T., 2007. DAI (DLM-1/ZBP1) is a cytosolic DNA sensor and an activator of innate immune response. Nature 448, 501–505.

Tarnopolsky, M., Kozenko, M., Jones, K., 2020. Expanding the phenotype: neurodevelopmental disorder, mitochondrial, with abnormal movements and lactic acidosis, with or without seizures (NEMMLAS) due to WARS2 biallelic variants, encoding mitochondrial tryptophanyl-tRNA synthase. J. Child Neurol. 35, 176–177.

Walsh, D., Mathews, M., Mohr, I., 2013. Tinkering with translation: protein synthesis in virus-infected cells. Cold Spring Harbor Perspect. Biol. 5, a012351.

Walsh, D., Mohr, I., 2011. Viral subversion of the host protein synthesis machinery. Nat. Rev. Microbiol. 9, 860–875.

Wang, J., Chu, B., Du, L., Han, Y., Zhang, X., Fan, S., Wang, Y., Yang, G., 2015. Molecular cloning and functional characterization of porcine cyclic GMP-AMP synthase. Mol. Immunol. 65, 436–445.

Wang, J., Liu, J.Y., Shao, K.Y., Han, Y.Q., Li, G.L., Ming, S.L., Su, B.Q., Du, Y.K., Liu, Z.H., Zhang, G.P., Yang, G.Y., Chu, B.B., 2019. Porcine reproductive and respiratory syndrome virus activates lipophagy to facilitate viral replication through downregulation of NDRG1 expression. J. Virol. 93, e00526-19.

Wang, J., Wang, C.F., Ming, S.L., Li, G.L., Zeng, L., Wang, M.D., Su, B.Q., Wang, Q., Yang, G.Y., Chu, B.B., 2020. Porcine IFITM1 is a host restriction factor that inhibits pseudorabies virus infection. Int. J. Biol. Macromol. 151, 1181–1193.

Wang, J., Zeng, L., Zhang, L., Guo, Z.Z., Lu, S.F., Ming, S.L., Li, G.L., Wan, B., Tian, K.G., Yang, G.Y., Chu, B.B., 2017. Cholesterol 25-hydroxylase acts as a host restriction factor on pseudorabies virus replication. J. Gen. Virol. 98, 1467–1476.

Wang, M., Sips, P., Khin, E., Rotival, M., Sun, X., Ahmed, R., Widjaja, A.A., Schafer, S., Yusoff, P., Choksi, P.K., Ko, N.S., Singh, M.K., Epstein, D., Guan, Y., Houstek, J., Mracek, T., Nuskova, H., Mikell, B., Tan, J., Pesce, F., Kolar, F., Bottolo, L., Mancini, M., Hubner, N., Pravenec, M., Petretto, E., Macrae, C., Cook, S.A., 2016. Wars2 is a determinant of angiogenesis. Nat. Commun. 7, 12061.

Wang, R., Li, K., 2012. Host factors in the replication of positive-strand RNA viruses. Chang Gung Med. J. 35, 111–124.

Wang, Y., Li, G.L., Qi, Y.L., Li, L.Y., Wang, L.F., Wang, C.R., Niu, X.R., Liu, T.X., Wang, J., Yang, G.Y., Zeng, L., Chu, B.B., 2022. Pseudorabies virus inhibits expression of liver X receptors to assist viral infection. Viruses 14, 514.

Wang, Z., Choi, M., Ban, T., Yanai, H., Negishi, H., Lu, Y., Tamura, T., Takaoka, A., Nishikura, K., Taniguchi, T., 2007. Regulation of innate immune responses by DAI (DLM-1/ZBP1) and other DNA-sensing molecules. Proc. Natl. Acad. Sci. U. S. A. 105, 5477–5482.

Wong, G., Lu, J., Zhang, W., Gao, G.F., 2019. Pseudorabies virus: a neglected zoonotic pathogen in humans? Emerg. Microbes Infect. 8, 150–154.

Wozniakowski, G., Samorek-Salamonowicz, E., 2015. Animal herpesviruses and their zoonotic potential for cross-species infection. Ann. Agric. Environ. Med. 22, 191–194.

Xiao, J., Li, W., Zheng, X., Qi, L., Wang, H., Zhang, C., Wan, X., Zheng, Y., Zhong, R., Zhou, X., Lu, Y., Li, Z., Qiu, Y., Liu, C., Zhang, F., Zhang, Y., Xu, X., Yang, Z., Chen, H., Zhai, Q., Wei, B., Wang, H., 2020. Targeting 7-dehydrocholesterol reductase integrates cholesterol metabolism and IRF3 activation to eliminate infection. Immunity 52, 109–122 e106.

Xie, L., Fang, L., Wang, D., Luo, R., Cai, K., Chen, H., Xiao, S., 2010. Molecular cloning and functional characterization of porcine DNA-dependent activator of IFN-regulatory factors (DAI). Dev. Comp. Immunol. 34, 293–299.

Xu, N., Zhang, Z.-F., Wang, L., Gao, B., Pang, D.-W., Wang, H.-Z., Zhang, Z.-L., 2012. A microfluidic platform for real-time and in situ monitoring of virus infection process. Biomicrofluidics 6, 34122.

Yang, X., Guan, H., Li, C., Li, Y., Wang, S., Zhao, X., Zhao, Y., Liu, Y., 2019. Characteristics of human encephalitis caused by pseudorabies virus: a case series study. Int. J. Infect. Dis. 87, 92–99.

Yao, P., Fox, P., 2013. Aminoacyl-tRNA synthetases in medicine and disease. EMBO Mol. Med. 5, 332–343.

Yeung, M., Jia, L., Yip, C., Chan, J., Teng, J., Chan, K., Cai, J., Zhang, C., Zhang, A., Wong, W., Kok, K., Lau, S., Woo, P., Lo, J., Jin, D., Shih, S., Yuen, K., 2018. Human tryptophanyl-tRNA synthetase is an IFN-γ-inducible entry factor for Enterovirus. J. Clin. Invest. 128, 5163–5177.

Yu, P., Fu, P., Zeng, L., Qi, L., Wang, Q., Yang, G., Li, H., Wang, J., Chu, B., Wang, M., 2022. EGCG restricts PRRSV proliferation by disturbing lipid metabolism. Microbiol. Spectr. 10, 02276-02221.

Zhu, T., Jiang, X., Xin, H., Zheng, X., Xue, X., Chen, J.L., Qi, B., 2021. GADD34-mediated dephosphorylation of eIF2alpha facilitates pseudorabies virus replication by maintaining de novo protein synthesis. Vet. Res. 52, 148.